# Enhancing the fidelity of two-qubit gates by measurements

Tuvia Gefen, Daniel Cohen, Itsik Cohen, and Alex Retzker
*Racah Institute of Physics, The Hebrew University of Jerusalem, Jerusalem 91904, Givat Ram, Israel*
(Received 4 May 2016; published 9 March 2017)

Dynamical decoupling techniques are the method of choice for increasing gate fidelities. While these methods have produced very impressive results in terms of decreasing local noise and increasing the fidelities of single-qubit operations, dealing with the noise of two-qubit gates has proven more challenging. The main obstacle is that the noise time scale is shorter than the two-qubit gate itself, so that refocusing methods do not work. We present a measurement- and feedback-based method to suppress two-qubit-gate noise, which cannot be suppressed by conventional methods. We analyze in detail this method for an error model, which is relevant for trapped-ion quantum information.

DOI: 10.1103/PhysRevA.95.032314

## I. INTRODUCTION

Quantum computers hold the promise to solve problems more efficiently than classical computers [1]. However, for a long time it remained unclear whether even conceptually a quantum computer could be constructed. One compelling reason is that even a minute error in each computational step would rapidly accumulate to a large error. Remarkably, the theory of quantum fault tolerance [2–5] showed that this intuition was wrong. Actually, in order for a quantum computer to output the correct result with an arbitrarily small probability of failure, each gate operation must only fail with a small probability below a certain threshold. Thus, the precise value of the error threshold is extremely important to the field of quantum computation. This has initiated an enormous effort to reduce gate infidelities below the fault-tolerance threshold. Very good results have been achieved in various platforms, in particular in trapped ions, nitrogen-vacancy (NV) centers in diamond, and superconducting devices [6–9]. Most of these fidelities were achieved with the help of dynamical decoupling.

The field of dynamical decoupling (DD) was born with Hahn's idea in 1950 [10] to refocus inhomogeneous broadening in nuclear magnetic resonance (NMR). This effect was named *spin echo* and is currently used in many areas of physics from atomic systems [11] to condensed matter [12]. The major results of this field have given us the ability to initialize, manipulate, and detect the state of a qubit with extremely high precision, and even more impressively, the coherence time of qubits was prolonged by many orders of magnitude.

Hahn's idea was expanded to tackle homogeneous broadening by using a pulse sequence which is nowadays termed CPMG [13,14]. Based on the CPMG pulse sequence, a large number of subtle modifications have been made, among which are quantum "bang-bang" control [15,16], Uhrig dynamical decoupling (UDD) [17], and composite pulses [18]. Moreover, it was realized that these pulse sequences are effective in dealing with quantum noise [15]. Furthermore, in the last few years the field of coherent control has joined forces with spin manipulation, yielding even more successful, but also more complicated, pulse sequences [19,20].

These methods have made it possible to exceed the fault-tolerance threshold for single-qubit gates [6,8]. However, in the case of two-qubit gates, this task remains challenging [6,8]. Most noise sources of the two-qubit gates are single-qubit noisy terms, possessing a sufficiently long correlation time, e.g., frequency and phase noise [21] and magnetic noise [22]. Therefore, dynamical decoupling has considerably improved two-qubit gate fidelities in various platforms, and utilizing refocusing techniques is expected to improve these fidelities even more in the near future [6,19,23–26]. On the other hand, the noise originating from laser or microwave amplitude fluctuations creates a noisy two-qubit term. In order to refocus this amplitude noise without damaging the entanglement process, one might employ composite pulses [27]. However, as this amplitude noise could have a shorter time scale than the gate duration [28], a naive composite pulse approach would not suffice. The amplitude noise therefore places a limitation on the fidelity of two-qubit gates that might impede future advances.

A future scenario might be that most errors are below the fault-tolerance threshold by more than an order of magnitude, but two-qubit gates still suffer from a dominant amplitude error that is above it. In this paper, we show that in this scenario, noisy two-qubit-gate fidelities can be enhanced by a sequence of measurements and feedback, regardless of the noise's correlation time. The general idea is based on the following reasoning: A faulty two-qubit gate could be used to realize a faulty two-qubit measurement. The measurement, however, could be repeated many times and reduce the infidelity substantially, resulting in a high-fidelity two-qubit measurement. At the next stage the high-fidelity two-qubit measurement could be utilized to create a high-fidelity two-qubit gate. These two steps are presented in Fig. 1, where Figs. 1(a) and 1(b) show the first and second steps, respectively. This general idea could be used in many architectures with different error models, e.g., NV centers in diamond and superconducting qubits. However, here we will concentrate on trapped-ion systems. This paper is structured as follows: the amplitude error in trapped ions is introduced; then we present our method and show that it can arbitrarily suppress this noise. We show a detailed fidelity analysis and give an example of another noise model relevant for NV centers.

## II. ENTANGLING GATES WITH TRAPPED IONS

Entangling gates with trapped ions are realized using the Mølmer-Sørensen (MS) scheme [6,29–36], which is

 

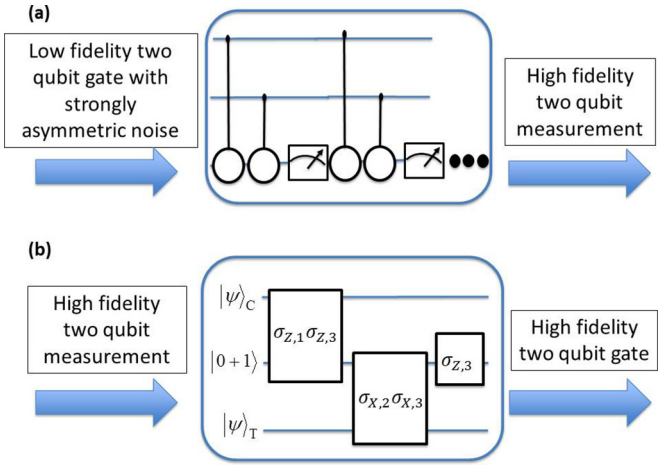


FIG. 1. The general scheme. The source of the protocol is a low-fidelity two-qubit gate with a specific error model with a single error operator. (a) The first step is to utilize this two-qubit gate together with single-qubit operations to create efficient two-qubit measurements, which are used in (b) the next step to create high-fidelity two-qubit gates.

constructed out of the following interaction:

$$H_{MS,i} = \Omega(\sigma_{x,i} + \sigma_{x,A})(b^\dagger e^{-i\delta t} + be^{i\delta t}), \tag{1}$$

where $b^\dagger$ ($b$) are the creation (annihilation) operators of the vibrational phonon, $\Omega$ is the sideband Rabi frequency, and $\delta = \omega_d - \nu$ is the detuning of the driving field from the secular frequency. During the MS gate operation, the two spins are entangled to the vibrational phonon, which generates the entanglement between the two spins. It is desirable to get a pure spin state, i.e., to keep the entanglement between the spins but to disentangle them from the phonons. This goal is indeed achieved, as after times of $\tau_{\text{gate}} = 2\pi n/\delta$ with integer $n$, the entanglement with the phonons is removed. In these times an effective Hamiltonian of $H = g\sigma_{X,1}\sigma_{X,2}$, where $g = \frac{\Omega^2}{\delta}$, is obtained. It is thus clear that in order to get a pure spin state, the accuracy of the gate duration $\tau_{\text{gate}}$ must be high. This accuracy is determined by the stability of the detuning $\delta$. Taking advantage of the low drift in the trap frequency and the high control of the driving frequency, the detuning $\delta$ remains stable during the experiment, and thus, dynamical decoupling techniques [27,37,38] can be used to disentangle the phonon from the spins.

Producing a pure spin state is also vulnerable to fluctuations of the Rabi frequency. These fluctuations may change the radius of the circle in the phonon phase space, such that even if the gate timing is accurate, there is a likelihood of not returning to the starting point; in other words, a phonon-spin entanglement may remain. Nevertheless, as long as these fluctuations are stable during a single circle, which is the case of the weak-coupling regime (high detuning), the phonon-spin entanglement is eliminated. In the strong-coupling regime, this noise makes only a second-order contribution, which is taken into account with the other noise terms that are not refocused.

However, the main source of decoherence originates from the first-order contribution of the fluctuating Rabi frequency. These fluctuations eventually give rise to an amplitude noise in the interaction: instead of realizing an effective Hamiltonian of $g\sigma_{X,1}\sigma_{X,2}$, the Hamiltonian $(g + \Delta g)\sigma_{X,i}\sigma_{X,A}$ is realized. Note that this argument also holds for other entangling gate schemes with trapped ions, such as the two-qubit phase gate [6,35,36]. In these two-qubit gates, in addition to the noisy interaction, the fluctuating Rabi frequency gives rise to a single-qubit noise, which can be refocused with regular dynamical decoupling techniques.

Thus, the noise in the interaction results in a faulty gate:

$$U_{MS} = \exp\left(-i\left[\frac{\pi}{4} + \varepsilon_i\right]\sigma_{x,1}\sigma_{x,2}\right),$$

where $\varepsilon_i$ denotes the error. We model $\varepsilon_i$ as a random variable uniformly distributed on $[-e,e]$. $U_{MS}$ is transformed to the controlled-NOT (CNOT) gate using single-qubit operations:

$$U_{Z,1}U_{X,2}U_{Y,1}U_{MS}U_{Y,1}^\dagger,$$

with $U_{\alpha,k} = \exp(-i\sigma_{\alpha,k}\pi/4)$ for $\alpha = x,y,z$ and $k = 1,2$. Assuming perfect single-qubit operations, the obtained gate is a perfect CNOT followed by an error of $\exp(i\varepsilon\sigma_{Z,1}\sigma_{X,2})$. The CNOT can be utilized to perform nonlocal measurements, for example. measurement of $\sigma_{Z,1}\sigma_{Z,2}$, i.e., parity detection, as shown in Fig. 1(a). The amplitude error will propagate through the CNOT gates to a final $\exp[i(\varepsilon_1\sigma_{Z,1} + \varepsilon_2\sigma_{Z,2})\sigma_{X,3}]$ error, which will result in an imperfect parity detection. This is illustrated by

$$\begin{aligned}
|0\rangle|0\rangle|0\rangle &\to \cos(\varepsilon_1+\varepsilon_2)|0\rangle|0\rangle|0\rangle - i\sin(\varepsilon_1+\varepsilon_2)|0\rangle|0\rangle|1\rangle,\\
|0\rangle|1\rangle|0\rangle &\to \cos(-\varepsilon_1+\varepsilon_2)|0\rangle|1\rangle|1\rangle + i\sin(-\varepsilon_1+\varepsilon_2)|0\rangle|1\rangle|0\rangle,\\
|1\rangle|0\rangle|0\rangle &\to \cos(\varepsilon_1-\varepsilon_2)|1\rangle|0\rangle|1\rangle + i\sin(\varepsilon_1-\varepsilon_2)|1\rangle|0\rangle|0\rangle,\\
|1\rangle|1\rangle|0\rangle &\to \cos(\varepsilon_1+\varepsilon_2)|1\rangle|1\rangle|0\rangle + i\sin(\varepsilon_1+\varepsilon_2)|1\rangle|1\rangle|1\rangle.
\end{aligned} \tag{2}$$

It can readily be observed that the error flips the ancilla, so that after the measurement there is still an overlap with states of the opposite parity. We will show that repeating the measurement many times reduces this overlap.

### The measurement scheme: From low-fidelity CNOT to high-fidelity measurement

The basic advantage of a measurement over a gate is that the measurement's fidelity can be increased by repeating it a few times, for example, detecting quantum jumps [39] or measuring one qubit via the ancilla [40]. We now show the validity of this argument in our case. It can be seen that the noise not only flips the ancilla but also causes a dephasing. Fortunately, states with the same parity have the same deformation up to a constant relative phase that can be corrected; hence, iteration is indeed useful. To illustrate, consider an initial state of $a|11\rangle + b|00\rangle + c|10\rangle + d|01\rangle$. Detection of 0, i.e., even parity, implies that we collapsed into $\cos(\varepsilon_1+\varepsilon_2)(a|11\rangle + b|00\rangle) + i\sin(\varepsilon_1-\varepsilon_2)(c|10\rangle - d|01\rangle)$, and detection of 1 implies that we collapsed into $i\sin(\varepsilon_1+\varepsilon_2)(a|11\rangle - b|00\rangle) + \cos(\varepsilon_1-\varepsilon_2)(c|10\rangle + d|01\rangle)$. As mentioned, there is an overlap with states of the opposite parity. If we now repeat the measurement three times and determine the parity according to a majority vote, the infidelity should go as $\sin(e)^4$ instead of $\sin(e)^2$. This is verified by a simple examination of the trajectories:

if the same outcome is obtained in all of the measurements, the overlap goes as $\sin(e)^3$, and the infidelity goes as $\sin(e)^6$, but there are still trajectories in which not all the outcomes are the same. In these trajectories the overlap goes as $\sin(e)$, but the probability of these trajectories goes as $\sin(e)^2$. Hence, altogether this accounts for an infidelity that goes as $\sin(e)^4$ instead of $\sin(e)^2$. This can be easily generalized to $2n-1$ repetitions: the worst-case scenario is an overlap that goes as $\sin(e)$, but the probability of these trajectories goes as $\sin(e)^{2n-2}$. Therefore, performing $2n-1$ iterations reduces the infidelity to an order of magnitude of $e^{2n}$.

Note that this measurement scheme can be further improved to take fewer operations. First, there is no need to apply two complete CNOT sequences in each iteration. It can be seen that the $\sigma_{X,1}\sigma_{X,2}$ measurement is performed by simply applying $M_{Z,3}U_{MS,23}U_{MS,13}$, where the third qubit is an ancilla. Therefore, the $\sigma_{Z,1}\sigma_{Z,2}$ measurement is realized by adding two Hadamard gates at the beginning of this sequence and two Hadamard gates at the end. Second, there is no need to perform all $2n-1$ repetitions in order to get a majority vote; we can end the sequence once any outcome is obtained $n$ times. Further analysis of this scheme will be presented in the upcoming sections.

## III. FROM HIGH-FIDELITY MEASUREMENT TO HIGH-FIDELITY CNOT

We now present our CNOT scheme, which employs two-qubit measurements and single-qubit operations. This scheme is depicted in Fig. 2 and is inspired by the scheme presented in [41]. This method consists of four qubits: control and target qubits, denoted as qubits 1 and 2, respectively, and two more ancillary qubits. One ancilla, denoted as qubit A1, is needed in order to be able to perform two-qubit measurements on the input qubits. They cannot be performed solely on the input, as the measurement might ruin the input state. The second ancilla, denoted as qubit A2, is needed to realize the two-qubit measurements. The scheme is as follows: the initial state of ancilla A1 is set to $\frac{1}{\sqrt{2}}|0+1\rangle_{A1}$, so we start with (neglecting normalization)

$$(\alpha|11\rangle_{1,2}+\beta|00\rangle_{1,2}+\gamma|10\rangle_{1,2}+\delta|01\rangle_{1,2})|0+1\rangle_{A1}|0\rangle_{A2}. \tag{3}$$

Now we measure $\sigma_{Z,1}\sigma_{Z,A1}$, for an outcome of a positive parity the state collapses into:

$$(\alpha|111\rangle_{1,2,A1}+\beta|000\rangle_{1,2,A1}+\gamma|101\rangle_{1,2,A1} +\delta|010\rangle_{1,2,A1})|0\rangle_{A2}, \tag{4}$$

while for a negative parity, a correction of $\sigma_{X,A1}$ is needed. In the next step we measure $\sigma_{X,2}\sigma_{X,A1}$. A positive parity would result in

$$(\alpha|1\rangle_1|11+00\rangle_{2,A1}+\beta|0\rangle_1|00+11\rangle_{2,A1} +\gamma|1\rangle_1|01+10\rangle_{2,A1}+\delta|0\rangle_1|10+01\rangle_{2,A1})|0\rangle_{A2}; \tag{5}$$

for a negative parity, again, a correction of $\sigma_{Z,1}\sigma_{Z,A1}$ is required. The last step is measuring ancilla A1. If we obtain $|0\rangle_{A1}$ the CNOT is realized; otherwise, we just need to apply a correction of $\sigma_{X,2}$. We remark that it would be more efficient to concentrate all the corrections at the end, instead of applying a correction after each measurement, as depicted in Fig. 2 and in Appendix A.

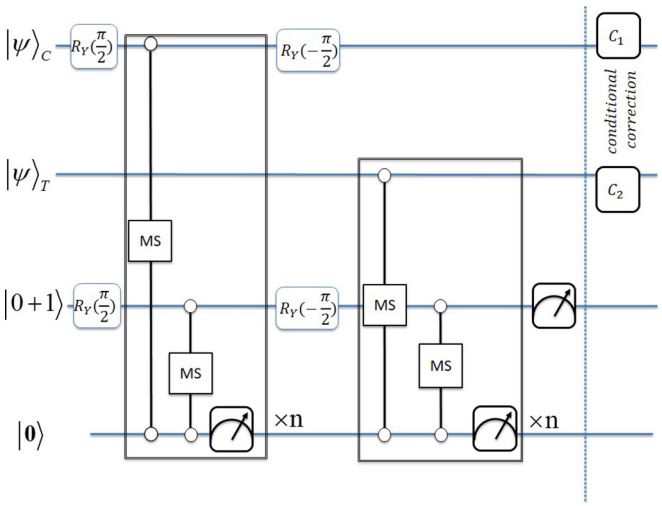


FIG. 2. A detailed description of the scheme that includes all the required qubits and operations. MS denotes the Mølmer-Sørensen gate. The first step is a $\sigma_{Z,1}\sigma_{Z,A1}$ measurement, the second is a $\sigma_{X,2}\sigma_{X,A1}$ measurement, and the last one is a $\sigma_{Z,A1}$ measurement. Depending on the measurement outcomes, a correction ($c_1$ and $c_2$ boxes) is applied on qubits 1 and 2.

Hence, a high-fidelity CNOT gate can be realized under the condition that a high-fidelity measurement can be realized. This specific example illustrates the main scenario in which there are high-fidelity operations, i.e., the single-qubit gates and measurements (which are below the threshold) and one low-fidelity operation: the CNOT gate (above the threshold). By utilizing many "cheap" operations we are able to increase the fidelity of the bad operation and bring it below the threshold.

We claim that this is the most efficient way to transform multiqubit measurements into a CNOT since one cannot produce a CNOT using one two-qubit measurement alone. This is quite clear: we can always choose a basis in which the operation of the measurement is not regular; that is, two orthogonal states are mapped to the same state. Thus, we cannot generate a CNOT utilizing only one two-qubit measurement and single qubit operations.

### Analysis

We first note that a parity measurement can be performed more efficiently. Instead of applying two CNOT gates, it is enough to realize the sequence

$$M_{Z,A1}U_{Y,2}U_{Y,1}U_{MS2,A1}U_{MS1,A1}U_{Y,2}^{\dagger}U_{Y,1}^{\dagger},$$

where $M_{Z,A1}$ denotes a measurement of the ancilla. Similarly, a measurement of $\sigma_{X,1}\sigma_{X,2}$ is realized by $M_{Z,3}U_{MS2,A1}U_{MS1,A1}$; in both cases a correction of a single-qubit operator is required according to the outcome. Let us first analyze the case in which the only errors are amplitude errors. Due to these errors the measurement is not accurate, and there is an overlap with states of the opposite parity. So given an initial state of $a|11\rangle+b|00\rangle+c|10\rangle+d|01\rangle$, if we detect an even parity, we collapse into $\cos(\varepsilon_1+\varepsilon_2)(a|11\rangle+b|00\rangle)+$

$\sin(\varepsilon_2-\varepsilon_1)(c|10\rangle+d|01\rangle)$, and detection of an odd parity implies that we collapse into $-\sin(\varepsilon_2+\varepsilon_1)(a|11\rangle+b|00\rangle)+\cos(\varepsilon_2-\varepsilon_1)(c|10\rangle+d|01\rangle)$. In order to decrease the infidelity, the measurement is repeated $2n-1$ times, and the outcome is determined according to a majority vote. We now want to calculate the average infidelity and show that if the infidelity of a single measurement goes as $e^2$, $2n-1$ repetitions yield infidelity that goes as $e^{2n}$. The average fidelity reads

$$\sum_{\varepsilon} p(\varepsilon)\sum_{\psi}\langle\psi(\varepsilon)|\psi(\varepsilon)\rangle|\langle\tilde{\psi}_p|\tilde{\psi}(\varepsilon)\rangle|, \tag{6}$$

where $|\psi(\varepsilon)\rangle$ is the unnormalized wave function given a specific measurement result, $|\tilde{\psi}(\varepsilon)\rangle$ is the normalized one, $|\tilde{\psi}_p\rangle$ is the normalized desired outcome, and $\varepsilon$ stands for all $\varepsilon_i$ involved in the CNOT. Equation (6) can be simplified to

$$\sum_{\psi,\varepsilon} p(\varepsilon)\langle\psi(\varepsilon)|\psi(\varepsilon)\rangle\sqrt{1-\frac{\langle\psi(\varepsilon)\Pi_r|\Pi_r\psi(\varepsilon)\rangle}{\langle\psi(\varepsilon)|\psi(\varepsilon)\rangle}}, \tag{7}$$

where $\Pi_r$ is the projection on the wrong subspace. Under the assumption that the probability of the odd subspace is of the same order of magnitude as the probability of the even subspace, which is indeed valid in all measurements performed in our CNOT, we get that $\frac{\langle\psi(\varepsilon)\Pi_r|\Pi_r\psi(\varepsilon)\rangle}{\langle\psi(\varepsilon)|\psi(\varepsilon)\rangle}\sim e$, and then taking the leading order of $e$ in Eq. (7), we get that the infidelity is

$$\frac{1}{2}\sum_{\psi,\varepsilon} p(\varepsilon)\langle\psi(\varepsilon)\Pi_r|\Pi_r\psi(\varepsilon)\rangle\approx\frac{1}{2}\binom{2n-1}{n}\left(\frac{2e^2}{3}\right)^n. \tag{8}$$

This expression is correct only in the leading order of $e$; a comparison with numerical values can be found in the Appendix A.

This is obviously not enough since we need to take into account other errors. We take the following error model: each single-qubit operation is followed by a single-qubit error with probability $e_2$, and each MS gate is followed by a single-qubit error with probability $2e_2$. There are clearly also detection errors which should be considered; we note that detection errors can be significantly suppressed by iteration and are thus taken to be $e_2$ (see Appendix A). We need to add the accumulation of these errors to the infidelity when $e_2$ is assumed to be below the threshold. Note that we can reduce the number of MS gates and therefore reduce the accumulation of these errors since not all the repetitions are required. Instead of making all $2n-1$ iterations, we just need to wait until one of the outcomes is repeated $n$ times. In the leading order of $e$ this yields the same infidelity as the $2n-1$ repetitions, but the average number of repetitions is reduced to $n(1+\frac{2e^2}{3})$ (Appendix A). The infidelity of the measurement thus reads

$$n\left(1+\frac{2e^2}{3}\right)5e_2+6e_2+\frac{1}{2}\binom{2n-1}{n}\left(\frac{2e^2}{3}\right)^n. \tag{9}$$

The infidelity of $\sigma_{X,i}\sigma_{X,j}$ is almost the same (it differs only in four Hadamard gates): $n(1+\frac{2e^2}{3})5e_2+2e_2+\frac{1}{2}(\frac{2n-1}{n})(\frac{2e^2}{3})^n$. We are now ready to obtain the infidelity of the CNOT. In addition to the errors in each of these two measurements, we have an error in the last measurement of the ancilla and errors in the last correction step. The infidelity of the CNOT is thus bounded by

$$\binom{2n-1}{n}\left(\frac{2e^2}{3}\right)^n+10n\left(1+\frac{2e^2}{3}\right)e_2+12e_2, \tag{10}$$

where this bound is indeed attained for certain states (Appendix A).

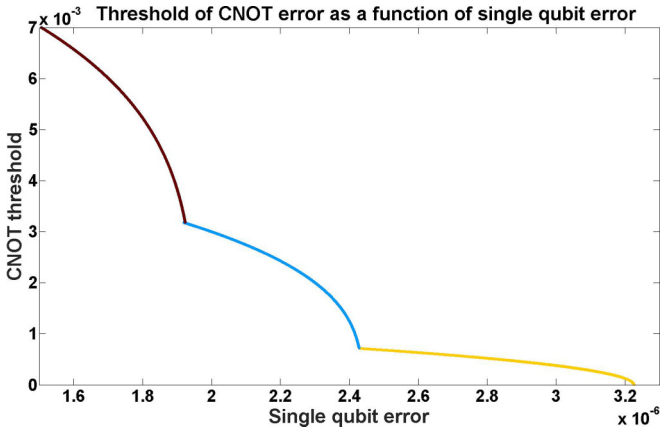


FIG. 3. Given a threshold $T$, the single-qubit error $e_2$ determines a new threshold for the original CNOT error, such that the infidelity of our CNOT will be below $T$. The plot shows this new threshold as a function of $e_2$ for $T=10^{-4}$. For each value of single-qubit error a different number of maximal repetitions is required: The brown (top) curve represents seven repetitions, the blue (middle) curve corresponds to five repetitions, and the yellow (bottom) curve represents three repetitions.

Therefore, given a fault-tolerance threshold $T$, which is unattainable for faulty two-qubit gates, the single-qubit error $e_2$ limits the number of repetitions that can be performed in order to reduce the error below $T$. The threshold of the original faulty CNOT as a function of $e_2$ is shown in Fig. 3 for $T=10^{-4}$.

We remark that this analysis might need modifications according to the exact experimental realization. Additional single-qubit operations may be required in order to cool the ions after measurements or shelve the ion states in order to ensure single addressing (see Appendix B).

We note that this method is useful for other noise models, for example, dephasing in one of the qubits. Since this is a dominant error in entangling gates in NV centers, this scheme could be relevant to this platform as well (see Appendix C).

## IV. CONCLUSIONS AND OUTLOOK

We presented a measurement-based method that increases the fidelity of entangling gates, which suffer from dominant amplitude error or dephasing noise. The scheme is based on the observation that these gates can be used for accurate measurements that can function as building blocks for the desired entangling gate. Note that some noise models seem to be resilient to this method, such as dephasing in both qubits, which leaves us with the question of whether there are similar methods for them.

## ACKNOWLEDGMENTS

A.R. acknowledges the support of the Israel Science Foundation (Grant No. 1500/13), the support of the European commission (STReP EQUAM Grant Agreement No. 323714), and the Niedersachsen-Israeli Research Cooperation Program and DIP program (FO 703/2-1). This work is partially supported by the US Army Research Office under Contract No. W911NF-15-1-0250.


## APPENDIX A: DETAILED ANALYSIS

Recall that the $\sigma_{Z,1}\sigma_{Z,2}$ measurement is performed in the following way:

$$M_{Z_{A2}} \exp\left(i\frac{\pi}{4}\sigma_{Y,2}\right)\exp\left(i\frac{\pi}{4}\sigma_{Y,1}\right) \times \exp\left(i\frac{\pi}{4}\sigma_{X,2}\sigma_{X,A2}\right)\exp\left(i\frac{\pi}{4}\sigma_{X,1}\sigma_{X,A2}\right)\cdot \times \exp\left(-i\frac{\pi}{4}\sigma_{Y,2}\right)\exp\left(-i\frac{\pi}{4}\sigma_{Y,1}\right), \tag{A1}$$

where $M_{Z_{A2}}$ denotes measurement of the third qubit (the ancilla) and a correction of $\sigma_{Z,1}$ follows any measurement of 1. Putting the amplitude error

$$M_{Z_{A2}} \exp\left(i\frac{\pi}{4}\sigma_{Y,2}\right)\exp\left(i\frac{\pi}{4}\sigma_{Y,1}\right) \times \exp\left[i\left(\frac{\pi}{4}+\varepsilon_2\right)\sigma_{X,2}\sigma_{X,A2}\right] \times \exp\left[i\left(\frac{\pi}{4}+\varepsilon_1\right)\sigma_{X,1}\sigma_{X,A2}\right] \times \exp\left(-i\frac{\pi}{4}\sigma_{Y,2}\right)\exp\left(-i\frac{\pi}{4}\sigma_{Y,1}\right) \tag{A2}$$

yields our imperfect measurement. Recall that $\varepsilon_i$ are modeled as identical random variables uniformly distributed between $-e$ and $e$. The effect of the amplitude error is illustrated by the following table:

$$\begin{aligned}
&|11\rangle|0\rangle \to i\cos(\varepsilon_1+\varepsilon_2)|11\rangle|1\rangle - \sin(\varepsilon_1+\varepsilon_2)|11\rangle|0\rangle,\\
&|10\rangle|0\rangle \to \cos(\varepsilon_1-\varepsilon_2)|10\rangle|0\rangle + i\sin(\varepsilon_1-\varepsilon_2)|10\rangle|1\rangle,\\
&|01\rangle|0\rangle \to \cos(\varepsilon_1-\varepsilon_2)|01\rangle|0\rangle - i\sin(\varepsilon_1-\varepsilon_2)|01\rangle|1\rangle,\\
&|00\rangle|0\rangle \to -i\cos(\varepsilon_1+\varepsilon_2)|00\rangle|1\rangle + \sin(\varepsilon_1+\varepsilon_2)|00\rangle|0\rangle.
\end{aligned} \tag{A3}$$

So given an initial state $a|11\rangle + b|00\rangle + c|10\rangle + d|01\rangle$, if we measure 1 (and make the repair), we collapse into

$$\cos(\varepsilon_1+\varepsilon_2)(a|11\rangle + b|00\rangle) + \sin(\varepsilon_2-\varepsilon_1)(c|10\rangle + d|01\rangle), \tag{A4}$$

and measuring 0, we collapse into

$$-\sin(\varepsilon_2+\varepsilon_1)(a|11\rangle + b|00\rangle) + \cos(\varepsilon_2-\varepsilon_1)(c|10\rangle + d|01\rangle). \tag{A5}$$

Note that because of the amplitude error, the measurement is not accurate, and there is an overlap with states of the opposite parity. This overlap goes as $\sin(e)$; thus, the infidelity of the measurement goes as $\sin(e)^2$. In order to decrease the infidelity, the measurement is repeated $2n-1$ times, and the outcome is determined according to a majority vote. Let us consider the case of three repetitions: if we get the same outcome in all three measurements, the undesired overlap will go as $\sin(e)^3$. Now measuring 1 three times consecutively will leave us with the nonnormalized state:

$$\cos(\varepsilon_1+\varepsilon_2)\cos(\varepsilon_3+\varepsilon_4)\cos(\varepsilon_5+\varepsilon_6)(a|11\rangle + b|00\rangle) + \sin(\varepsilon_2-\varepsilon_1)\sin(\varepsilon_4-\varepsilon_3)\sin(\varepsilon_6-\varepsilon_5)(c|10\rangle + d|01\rangle), \tag{A6}$$

and thus, the undesired overlap will be reduced. Regarding the case of different outcomes, for example, two 1s and one 0, we obtain the following nonnormalized state:

$$-\cos(\varepsilon_1+\varepsilon_2)\cos(\varepsilon_3+\varepsilon_4)\sin(\varepsilon_5+\varepsilon_6)(a|11\rangle + b|00\rangle) + \sin(\varepsilon_2-\varepsilon_1)\sin(\varepsilon_4-\varepsilon_3)\cos(\varepsilon_6-\varepsilon_5)(c|10\rangle + d|01\rangle). \tag{A7}$$

After normalization the undesired overlap goes as $\sin(e)$, but the probability for this trajectory goes as $\sin(e)$; altogether, this accounts for an infidelity that goes as $\sin(e)^4$ instead of $\sin(e)^2$.

We would now like to make a more precise calculation of the average fidelity of this measurement, given a certain number of repetitions. We wish to show that for a single measurement with an infidelity that goes as $e^2$, then $2n-1$ repetitions yield an infidelity that goes as $e^{2n}$.

The average fidelity reads

$$\sum_{\varepsilon} p(\varepsilon)\sum_{\psi}\langle\psi(\varepsilon)|\psi(\varepsilon)\rangle|\langle\tilde{\psi}_p|\tilde{\psi}(\varepsilon)\rangle|, \tag{A8}$$

where $|\psi(\varepsilon)\rangle$ is the unnormalized wave function given a specific measurement result, $|\tilde{\psi}(\varepsilon)\rangle$ is the normalized one, $|\tilde{\psi}_p\rangle$ is the normalized desired outcome, and we observe that $|\tilde{\psi}_p\rangle = \frac{\Pi_c|\psi(\varepsilon)\rangle}{\sqrt{\langle\psi(\varepsilon)\Pi_c|\Pi_c\psi(\varepsilon)\rangle}}$, where $\Pi_c$ is the projection on the correct subspace and $\Pi_r$ is the projection on the wrong subspace. Hence, the average fidelity reads

$$\sum_{\psi,\varepsilon} p(\varepsilon)\sqrt{\langle\psi(\varepsilon)\Pi_c|\Pi_c\psi(\varepsilon)\rangle\langle\psi(\varepsilon)|\psi(\varepsilon)\rangle}. \tag{A9}$$

The average fidelity is thus larger than $\sum_{\psi,\varepsilon} p(\varepsilon)\langle\psi(\varepsilon)\Pi_c|\Pi_c\psi(\varepsilon)\rangle$, and therefore, the infidelity is bounded by $\sum_{\psi,\varepsilon} p(\varepsilon)\langle\psi(\varepsilon)\Pi_r|\Pi_r\psi(\varepsilon)\rangle$. This bound is the same for any initial state, and in the case of three repetitions we have $\sum_{\psi,\varepsilon} p(\varepsilon)\langle\psi(\varepsilon)\Pi_r|\Pi_r\psi(\varepsilon)\rangle = S(e)^3 + \binom{3}{2}C(e)S(e)^2$, where $C(e) = \frac{1}{4e^2}\int_{-e}^{e}\int_{-e}^{e}\cos^2(x+y)dxdy \sim 1 - \frac{2e^2}{3}$ and $S(e) = \frac{1}{4e^2}\int_{-e}^{e}\int_{-e}^{e}\sin^2(x+y)dxdy \sim \frac{2e^2}{3}$. Hence, for three repetitions we get that the infidelity is bounded by $3\left(\frac{2e^2}{3}\right)^2$, and for $n$ repetitions it is bounded by $\binom{n}{\frac{n+1}{2}}\left(\frac{2e^2}{3}\right)^{\frac{n+1}{2}}$. This bound is attained for any initial state that lies in only one of the subspaces (any initial state with a well-defined parity). This is because in this case for any trajectory that gives the correct parity $\Pi_c|\psi(\varepsilon)\rangle = |\psi(\varepsilon)\rangle, \Pi_r|\psi(\varepsilon)\rangle = 0$, and for any trajectory that gives the wrong parity $\Pi_r|\psi(\varepsilon)\rangle = |\psi(\varepsilon)\rangle, \Pi_c|\psi(\varepsilon)\rangle = 0$. However, in the case where $|a|^2 + |b|^2$ is of the same order of magnitude as $|c|^2 + |d|^2$, the infidelity will be smaller than the bound. We

now calculate the infidelity in this case: note that Eq. (A9) can be written as

$$\sum_{\psi,\varepsilon} p(\varepsilon)\sqrt{\langle\psi(\varepsilon)|\psi(\varepsilon)\rangle^2 - \langle\psi(\varepsilon)\Pi_r|\Pi_r\psi(\varepsilon)\rangle\langle\psi(\varepsilon)|\psi(\varepsilon)\rangle}, \tag{A10}$$

which can be simplified to

$$\sum_{\psi,\varepsilon} p(\varepsilon)\langle\psi(\varepsilon)|\psi(\varepsilon)\rangle\sqrt{1-\frac{\langle\psi(\varepsilon)\Pi_r|\Pi_r\psi(\varepsilon)\rangle}{\langle\psi(\varepsilon)|\psi(\varepsilon)\rangle}}. \tag{A11}$$

Under the assumption that $|a|^2+|b|^2$ has the same order of magnitude as $|c|^2+|d|^2$, then $\frac{\langle\psi(\varepsilon)\Pi_r|\Pi_r\psi(\varepsilon)\rangle}{\langle\psi(\varepsilon)|\psi(\varepsilon)\rangle}\sim e$, and then taking the leading order of $e$ in Eq. (A11), we get that the infidelity is

$$\frac{1}{2}\sum_{\psi,\varepsilon} p(\varepsilon)\langle\psi(\varepsilon)\Pi_r|\Pi_r\psi(\varepsilon)\rangle \approx \frac{1}{2}\binom{n}{\frac{n+1}{2}}\left(\frac{2e^2}{3}\right)^{\frac{n+1}{2}}. \tag{A12}$$

We can compare this approximation to numerical values for $e=0.3$ and $|a|^2+|b|^2=|c|^2+|d|^2$:

| | Three repetitions | Five repetitions |
|---|---|---|
| Numerical | 0.0058 | 0.001 37 |
| Approximated | 0.0054 | 0.001 08 |

We also need to take into account other single-qubit errors that are assumed to be below the threshold. The other sources of error are single-qubit operations and measurements. The measurement infidelity can be substantially reduced by iteration; the only limitation here is the finite coherence time of the qubit that limits the number of iterations. It would therefore be reasonable to assume that the measurement error is upper bounded by the single-qubit gate's error; this is justified and discussed in the next section. As for the single-qubit gates, we assume the following noise model: each single-qubit rotation of $\frac{\pi}{4}$ is followed by a single-qubit error with probability $e_2$, and any MS gate is followed by a single-qubit error with probability $e_2$ on each of the relevant two qubits. Now $2n-1$ iterations of $\sigma_{Z,i}\sigma_{Z,j}$ measurement include $4n-2$ MS gates, $2n-1$ detections, four Hadamard gates, one correction of $\frac{\pi}{2}$ rotations with probability $\frac{1}{2}$, and one measurement to initialize the ancilla. We thus get that the infidelity of this measurement reads $(10n+1)e_2+\frac{1}{2}(\frac{2n-1}{n})(\frac{2e^2}{3})^n$.

But, as mentioned in the main text, the number of single-qubit errors can be significantly reduced, as we do not need all $2n-1$ repetitions. Recall that $2n-1$ repetitions are used to lower the amplitude error from $e$ to $e^n$. But in order to get this improvement we just need to wait until one of the outcomes is repeated $n$ times, and in most cases this will require less than $2n-1$ repetitions. So a more efficient scheme is to repeat the measurement until one of the outcomes occurs $n$ times; in the leading order of $e$, the same infidelity is achieved (taking into account only the amplitude errors). Note that the probability to stop after $k$ repetitions ($n\leqslant k\leqslant 2n-1$) is $(\frac{n+k-1}{k})[C(e)^nS(e)^k+S(e)^nC(e)^k]$; thus, the average stopping time is given by $\sum_{k=0}^{n-1}k(\frac{n+k-1}{k})[p^n(1-p)^k+p^k(1-p)^n]$, which goes as $n[1+S(e)]$. Hence, the probability for a single-qubit error is now $\{5n[1+S(e)]+6\}e_2$, and the infidelity reads

$$\left[5n\left(1+\frac{2e^2}{3}\right)+6\right]e_2+\frac{1}{2}\binom{2n-1}{n}\left(\frac{2e^2}{3}\right)^n. \tag{A13}$$

We now want to calculate the average infidelity of the entire CNOT. The imperfect $\sigma_{X,1}\sigma_{X,2}$ measurement yields the following outcomes:

Collapsing into $|0\rangle$ (so we do not need to perform a correction),

$$\begin{aligned}
|11\rangle &\to \cos(\varepsilon_1-\varepsilon_2)|11-00\rangle-\sin(\varepsilon_1+\varepsilon_2)|11+00\rangle,\\
|10\rangle &\to \cos(\varepsilon_1-\varepsilon_2)|10-01\rangle-\sin(e1+e2)|10+01\rangle,\\
|01\rangle &\to \cos(\varepsilon_1-\varepsilon_2)|01-10\rangle-\sin(\varepsilon_1+\varepsilon_2)|01+10\rangle,\\
|00\rangle &\to \cos(\varepsilon_1-\varepsilon_2)|00-11\rangle-\sin(\varepsilon_1+\varepsilon_2)|00+11\rangle.
\end{aligned}$$

Collapsing into $|1\rangle$ (and applying $\sigma_{X,1}$ correction),

$$\begin{aligned}
|11\rangle &\to \cos(\varepsilon_1+\varepsilon_2)|11+00\rangle+\sin(\varepsilon_2-\varepsilon_1)||11-00\rangle,\\
|10\rangle &\to \cos(\varepsilon_1+\varepsilon_2)|10+01\rangle+\sin(\varepsilon_2-\varepsilon_1)|10-01\rangle,\\
|01\rangle &\to \cos(\varepsilon_1+\varepsilon_2)|01+10\rangle+\sin(\varepsilon_2-\varepsilon_1)|01-10\rangle,\\
|00\rangle &\to \cos(\varepsilon_1+\varepsilon_2)|00+11\rangle+\sin(\varepsilon_2-\varepsilon_1)|00-11\rangle.
\end{aligned}$$

The infidelity analysis of this measurement is obviously similar to that of the $\sigma_{Z,1}\sigma_{Z,2}$ measurement, except that one does not need the four Hadamard gates, so the infidelity of this measurement is $[5n(1+\frac{2e^2}{3})+2]e_2+\frac{1}{2}(\frac{2n-1}{n})(\frac{2e^2}{3})^n$.

We are now poised to get the CNOT infidelity. To this end, we need to understand how the $\sigma_Z\sigma_Z$ and $\sigma_X\sigma_X$ measurement errors propagate. Let us examine this for the $\sigma_{Z,1}\sigma_{Z,A1}$ measurement:

$$(\alpha|11\rangle+\beta|00\rangle+\gamma|10\rangle+\delta|01\rangle)|1+0\rangle \tag{A14}$$

will become after the measurement

$$\begin{aligned}
&r(\varepsilon)(\alpha|111\rangle+\beta|000\rangle+\gamma|101\rangle+\delta|010\rangle)\\
&\quad+\varepsilon(\alpha|110\rangle+\beta|001\rangle+\gamma|100\rangle+\delta|011\rangle),
\end{aligned} \tag{A15}$$

where $r(\varepsilon)$ denotes the relevant normalization factor. After a flawless $\sigma_{X,2}\sigma_{X,A1}$ measurement (and repair if necessary) and a $\sigma_{Z,A1}$ measurement (and repair if necessary) we get

$$\begin{aligned}
&r(\varepsilon)(\alpha|10\rangle+\beta|00\rangle+\gamma|11\rangle+\delta|01\rangle)\\
&\quad+\varepsilon(\alpha|11\rangle+\beta|01\rangle+\gamma|10\rangle+\delta|00\rangle).
\end{aligned} \tag{A16}$$

Hence, the $\sigma_{Z,1}\sigma_{Z,A1}$ error corresponds to an $\sigma_{X,2}$ error.

Considering the $\sigma_{X,A1}\sigma_{X,2}$ error,

$$\alpha|111\rangle+\beta|000\rangle+\gamma|101\rangle+\delta|010\rangle \tag{A17}$$

will become after the measurement

$$\begin{aligned}
&r(\varepsilon)[\alpha|1(11+00)\rangle+\beta|0(00+11)\rangle\\
&\quad+\gamma|1(10+01)\rangle+\delta|0(01+10)\rangle]\\
&\quad+\varepsilon[\alpha|1(11-00)\rangle+\beta|0(00-11)\rangle\\
&\quad+\gamma|1(01-10)\rangle+\delta|0(10-01)\rangle].
\end{aligned} \tag{A18}$$

And after measurement of $\sigma_{Z,A1}$

$$\begin{aligned}
&r(\varepsilon)(\alpha|10\rangle+\beta|00\rangle+\gamma|11\rangle+\delta|01\rangle)\\
&\quad+\varepsilon(-\alpha|10\rangle+\beta|00\rangle-\gamma|11\rangle+\delta|01\rangle).
\end{aligned} \tag{A19}$$

Hence, the $\sigma_{X,A1}\sigma_{X,2}$ error corresponds to a $\sigma_{Z,1}$ error. So after neglecting the terms that correspond to error in both measurements, we get

$$\begin{aligned} & r(\varepsilon_1,\varepsilon_2)(\alpha|10\rangle+\beta|00\rangle+\gamma|11\rangle+\delta|01\rangle) \\ & +\varepsilon_1(\alpha|11\rangle+\beta|01\rangle+\gamma|10\rangle+\delta|00\rangle) \\ & +\varepsilon_2(-\alpha|10\rangle+\beta|00\rangle-\gamma|11\rangle+\delta|01\rangle). \end{aligned} \quad \text{(A20)}$$

In the leading order of $e$, the infidelity equals $\frac{1}{2}\sum_{\psi,\varepsilon} p(\varepsilon_1,\varepsilon_2)\langle\psi(\varepsilon_1,\varepsilon_2)\Pi_r|\Pi_r\psi(\varepsilon_1,\varepsilon_2)\rangle$. So this is just

$$\begin{aligned} & \sum_{\varepsilon} p(\varepsilon_1,\varepsilon_2)[(\varepsilon_1)^2(1-|\langle\psi|\psi_1\rangle|^2)+(\varepsilon_2)^2(1-|\langle\psi|\psi_2\rangle|^2) \\ & +\varepsilon_1\varepsilon_2(\langle\psi_2|\psi_1\rangle+\langle\psi_1|\psi_2\rangle-\langle\psi_1|\psi\rangle\langle\psi|\psi_2\rangle \\ & -\langle\psi_2|\psi\rangle\langle\psi|\psi_1\rangle)]. \end{aligned} \quad \text{(A21)}$$

Now we note that $\langle\varepsilon_1\varepsilon_2\rangle=\langle\varepsilon_1\rangle\langle\varepsilon_2\rangle=0$. So we are left with

$$\langle(\varepsilon_1)^2\rangle(1-|\langle\psi|\psi_1\rangle|^2)+\langle(\varepsilon_2)^2\rangle(1-|\langle\psi|\psi_2\rangle|^2), \quad \text{(A22)}$$

but we already calculated $\langle(\varepsilon_1)^2\rangle,\langle(\varepsilon_2)^2\rangle$: this is simply the infidelity of the measurement. Hence, in the leading order of $e$, the fidelity of the CNOT is

$$\begin{aligned} & \varepsilon[2-(|\beta|^2+|\delta|^2-|\alpha|^2-|\gamma|^2)^2 \\ & -(\alpha^*\delta+\delta^*\alpha+\beta^*\gamma+\gamma^*\beta)^2], \end{aligned} \quad \text{(A23)}$$

where $\varepsilon$ denotes the measurement infidelity. Note that by taking, for example, $\alpha=\frac{1}{2},\delta=\frac{i}{2},\beta=\frac{1}{2},\gamma=\frac{i}{2}$, the infidelity is just $2\varepsilon$. As noted in the main text single-qubit corrections should be applied in the case of wrong measurement outcomes. As we have just seen, a wrong outcome in the $\sigma_{Z,1}\sigma_{Z,A1}$ measurement is transformed into a final $\sigma_{X,2}$ error. A wrong measurement outcome in the $\sigma_{X,2}\sigma_{X,A1}$ measurement is transformed to a final $\sigma_{Z,1}$ error, and it can be easily seen that a wrong outcome in the $\sigma_{Z,A1}$ measurement is also transformed to a $\sigma_{Z,1}$ error. Hence, wrong outcomes in the first and last measurements cancel each other. Recall that we need also to add an $e_2$ error due to the last measurement. This accounts for an additional $4e_2$ term in the infidelity (in fact $3\frac{1}{4}e_2$). Therefore, the total infidelity of the CNOT as a function of $n$, the required majority vote, reads

$$\left[10n\left(1+\frac{2e^2}{3}\right)+12\right]e_2+\binom{2n-1}{n}\left(\frac{2e^2}{3}\right)^n. \quad \text{(A24)}$$

Equation (A24) tells us that the problem of decreasing the infidelity of the CNOT is mapped to the problem of reducing the single-qubit errors $e_2$. If $e_2$ is small enough, we can take as many iterations as needed, thereby reducing the amplitude error below the threshold. Given a threshold $T$, any $e_2$ limits the number of iterations and thus imposes a new threshold for the original CNOT error. This is shown in Fig. 3 in the main text. Note that the original CNOT error is $\frac{1}{2}\frac{1}{2e}\int_{-e}^{e}\sin^2(x)dx=\frac{e^2}{6}$; thus, the infidelity of our CNOT as a function of the original mean CNOT error (denoted as $e'$) is

$$[10n(1+4e')+12]e_2+\binom{2n-1}{n}(4e')^n. \quad \text{(A25)}$$

*The length of the gate and decoherence.* An additional source of error is the limited coherence time of the qubits. We must make sure that the duration of the scheme is much shorter than the coherence time. Let us perform this analysis. A coherence time of 50 s was already achieved with hyperfine qubits [42]. Currently, single-qubit rotations and Ms gates take about 2 and 30 $\mu$s, respectively [9]. Measurement is the longest operation in our scheme, as state-of-the-art measurements take about 330 $\mu$s with an error of $2\times10^{-3}$ [9]. By taking a majority vote of 2 the error is reduced to $1.2\times10^{-5}$, and the average duration is about 660 $\mu$s. With a majority vote of 3 the error is $8\times10^{-8}$, and the average duration is 990 $\mu$s. So we are now poised to get the total duration of the scheme: for a majority vote of $n$ (in both measurements) it includes about $4n$ MS gates and about $2n+1$ measurements. Since there are only six single-qubit gates and they are much shorter, they can be neglected. Hence, the duration (in microseconds) is about $(2n+1)30+(4n)330$. For $n=2,3,4$, i.e., 3,5,7 repetitions, the duration is 2.7, 7.3, 9.4 ms, respectively. Comparing these to the coherence time ($\sim$50 s), we get that the infidelities due to decoherence are $\sim10^{-8}$. Therefore, this should not cause a concern to our scheme. In fact, even if we take a coherence time of 2 s, which was achieved for Zeeman qubits [43], we get that the infidelity due to decoherence is $\sim10^{-6}$ (for a majority vote of 2), which does not affect the scheme.

## APPENDIX B: POSSIBLE MODIFICATIONS TO THE ANALYSIS

The analysis above may change according to the details of the experimental realization. The multiple measurements may heat up the ions and thus introduce additional errors; this can be overcome by performing sympathetic cooling [44] after every measurement. This means adding on average $2n(1+4e)+1$ more operations. Assuming the error in each of these operations is $e_2$, the infidelity would change to $[12n(1+4e)+13]e_2+(\frac{2n-1}{n})(4e)^n$, which is quite a minor change. Another possible issue is the need for single addressing of each of the ions. This should not pose a problem if the addressing error can be reduced to $\sim10^{-6}$, as Ref. [45] suggests. Otherwise, shelving gates are required, i.e., mapping the qubits on which we wish to operate to different states. Let us consider the worst-case scenario, in which shelving is needed in any MS gate, single-qubit gates, and measurements. Then a shelving gate is performed before and after each of these operations; this leads to $20n(1+4e)+24$ more single-qubit gates, so the infidelity reads $[30n(1+4e')+36]e_2+(\frac{2n-1}{n})(4e')^n$. This indeed increases the infidelity, but still a significant improvement can be achieved for $e_2\sim10^{-6}$. In that case the minimal $e_2$ required for an improvement is $e_2=1.04\times10^{-6}$, and for $e_2=10^{-6}$ we already get that an original CNOT error of $5\times10^{-4}$ can be lowered to $10^{-4}$. We note that this should not have a big effect on the length of the scheme, as single-qubit gates take only 2 $\mu$s, and thus, introducing shelving increases the length by just $\sim100$ $\mu$s, which is acceptable.

## APPENDIX C: RELEVANCE TO NV CENTERS AND OTHER NOISE MODELS

This method can be applied to other noise models as well, in particular to dephasing in one of the qubits. Namely, instead of realizing a Hamiltonian of $g\sigma_{Z,1}\sigma_{Z,2}$, we get $g\sigma_{Z,1}\sigma_{Z,2}+\varepsilon\sigma_{Z,1}$. This noise again induces a syndrome measurement mistake and thus can be suppressed by iteration.

This noise model is the dominant error in entangling gates in NV centers. In this platform the main source of decoherence is a slow drift in the NV energy gap, and this is the undesired $\varepsilon\sigma_{Z,2}$. When using these gates for parity measurements, this noise term flips the ancilla and changes the measurement's result; thus, the measurement-feedback method works.

It should be noted that for other noise models such as dephasing in both qubits, our method is not useful since the error not only changes the syndrome but also deforms the superposition. A future challenge would be to examine whether a similar method can be used to suppress this kind of noise.


[1] P. W. Shor, Scheme for reducing decoherence in quantum computing memory, Phys. Rev. A **52**, R2493 (1995).

[2] E. Knill, R. Laflamme, and W. Zurek, Accuracy threshold for quantum computation, Los Alamos National Laboratory, Technical Report LAUR-96-2199 LANL, 1996 (unpublished).

[3] D. Aharonov and M. Ben-Or, in *Proceedings of the 29th ACM Symposium on Theory of Computing* (Association for Computing Machinery, New York, 1997), p. 176.

[4] A. Yu. Kitaev, Fault-tolerant quantum computation by anyons, Ann. Phys. (NY) **303**, 2 (2003).

[5] P. Aliferis, D. Gottesman, and J. Preskill, Quantum accuracy threshold for concatenated distance-3 codes, Quantum Inf. Comput. **6**, 97 (2006).

[6] C. J. Ballance, T. P. Harty, N. M. Linke, M. A. Sepiol, and D. M. Lucas, High-Fidelity Quantum Logic Gates Using Trapped-Ion Hyperfine Qubits, Phys. Rev. Lett. **117**, 060504 (2016).

[7] R. Barends, J. Kelly, A. Megrant, A. Veitia, D. Sank, E. Jeffrey, T. C. White, J. Mutus, A. G. Fowler, B. Campbell, Y. Chen, Z. Chen, B. Chiaro, A. Dunsworth, C. Neill, P. OMalley, P. Roushan, A. Vainsencher, J. Wenner, A. N. Korotkov, A. N. Cleland, and J. M. Martinis, Superconduting quantum circuits at the surface code threshold for fault tolerance, Nature (London) **508**, 500 (2014).

[8] X. Rong, J. Geng, F. Shi, Y. Liu, K. Xu, W. Ma, F. Kong, Z. Jiang, Y. Wu, and J. Du, Experimental fault-tolerant universal quantum gates with solid-state spins under ambient conditions, Nat. Commun. **6**, 8748 (2015).

[9] J. P. Gaebler, T. R. Tan, Y. Lin, Y. Wan, R. Bowler, A. C. Keith, S. Glancy, K. Coakley, E. Knill, D. Leibfried, and D. J. Wineland, High-Fidelity Universal Gate Set for $^{9}Be^{+}$ Ion Qubits, Phys. Rev. Lett. **117**, 060505 (2016).

[10] E. L. Hahn, Spin Echoes, Phys. Rev. **80**, 580 (1950).

[11] M. J. Biercuk, H. Uys, A. P. VanDevender, N. Shiga, W. M. Itano, and J. J. Bollinger, Optimized dynamical decoupling in a model quantum memory, Nature (London) **458**, 996 (2009).

[12] B. Naydenov, F. Dolde, L. T. Hall, C. Shin, H. Fedder, L. C. L. Hollenberg, F. Jelezko, and J. Wrachtrup, Dynamical decoupling of a single-electron spin at room temperature, Phys. Rev. B **83**, 081201(R) (2011).

[13] H. Y. Carr and E. M. Purcell, Effects of diffusion on free precession in nuclear magnetic resonance experiments, Phys. Rev. **94**, 630 (1954).

[14] S. Meiboom and D. Gill, Modified spinecho method for measuring nuclear relaxation times, Rev. Sci. Inst. **29**(8), 688 (1958).

[15] L. Viola and S. Lloyd, Dynamical suppression of decoherence in two-state quantum systems, Phys. Rev. A **58**, 2733 (1998).

[16] L. Viola, E. Knill, and S. Lloyd, Dynamical Decoupling of Open Quantum Systems, Phys. Rev. Lett. **82**, 2417 (1999).

[17] G. S. Uhrig, Keeping a Quantum Bit Alive by Optimized-Pulse Sequences, Phys. Rev. Lett. **98**, 100504 (2007).

[18] K. R. Brown, A. W. Harrow, and I. L. Chuang, Arbitrarily accurate composite pulse sequences, Phys. Rev. A **70**, 052318 (2004).

[19] N. Timoney, V. Elman, S. Glaser, C. Weiss, M. Johanning, W. Neuhauser, and C. Wunderlich, Error-resistant single-qubit gates with trapped ions, Phys. Rev. A **77**, 052334 (2008).

[20] S. Montangero, T. Calarco, and R. Fazio, Robust Optimal Quantum Gates for Josephson Charge Qubits, Phys. Rev. Lett. **99**, 170501 (2007).

[21] M. Bishof, X. Zhang, M. J. Martin, and J. Ye, Optical Spectrum Analyzer with Quantum-Limited Noise Floor, Phys. Rev. Lett. **111**, 093604 (2013).

[22] S. Kotler, N. Akerman, Y. Glickman, A. Keselman, and R. Ozeri, Single Ion quantum lock-in amplifier, Nature (London) **473**, 61 (2011).

[23] M. J. Biercuk, H. Uys, A. P. VanDevender, N. Shiga, W. M. Itano, and J. J. Bollinger, Experimental Uhrig dynamical decoupling using trapped ions, Phys. Rev. A **79**, 062324 (2009).

[24] T. R. Tan, J. P. Gaebler, R. Bowler, Y. Lin, J. D. Jost, D. Leibfried, and D. J. Wineland, Demonstration of a Dressed-State Phase Gate for Trapped Ions, Phys. Rev. Lett. **110**, 263002 (2013).

[25] S. C. Webster, S. Weidt, K. Lake, J. J. McLoughlin, and W. K. Hensinger, Simple Manipulation of a Microwave Dressed-State Ion Qubit, Phys. Rev. Lett. **111**, 140501 (2013).

[26] N. Timoney, I. Baumgart, M. Johanning, A. F. Varon, Ch. Wunderlich, M. B. Plenio, and A. Retzker, Quantum gates and memory using microwave dressed states, Nature (London) **476**, 185 (2011).

[27] S. S. Ivanov and N. V. Vitanov, Composite two-qubit gates, Phys. Rev. A **92**, 022333 (2015).

[28] I. Cohen, A. Rotem, and A. Retzker, Refocusing two-qubit-gate noise for trapped ions by composite pulses, Phys. Rev. A **93**, 032340 (2016).

[29] A. Sorensen and K. Molmer, Quantum Computation with Ions in Thermal Motion, Phys. Rev. Lett. **82**, 1971 (1999).

[30] C. A. Sackett, D. Kielpinski, B. E. King, C. Langer, V. Meyer, C. J. Myatt, M. Rowe, Q. A. Turchette, W. M. Itano, D. J. Wineland, and C. Monroe, Experimental entanglement of four particles, Nature (London) **404**, 256 (2000).

[31] J. Benhelm, G. Kirchmair, C. F. Roos, and R. Blatt, Towards fault-tolerant quantum computing with trapped ions, Nat. Phys. **4**, 463 (2008).

[32] K. Kim, M.-S. Chang, R. Islam, S. Korenblit, L.-M. Duan, and C. Monroe, Entanglement and Tunable Spin-Spin Couplings between Trapped Ions Using Multiple Transverse Modes, Phys. Rev. Lett. **103**, 120502 (2009).

[33] N. Navon, N. Akerman, S. Kotler, Y. Glickman, and R. Ozeri, Quantum process tomography of a Mølmer-Sørensen interaction, Phys. Rev. A **90**, 010103(R) (2014).

[34] T. R. Tan, J. P. Gaebler, Y. Lin, Y. Wan, R. Bowler, D. Leibfried, and D. J. Wineland, Multi-element logic gates for trapped-ion qubits, Nature (London) **528**, 380 (2015).

[35] D. Leibfried, B. DeMarco, V. Meyer, D. Lucas, M. Barrett, J. Britton, W. M. Itano, B. Jelenković, C. Langer, T. Rosenband, and D. J. Wineland, Experimental demonstration of a robust, high-fidelity geometric two ion-qubit phase gate, Nature (London) **422**, 412 (2003).

[36] C. J. Ballance, V. M. Schafer, J. P. Home, D. J. Szwer, S. C. Webster, D. T. C. Allcock, N. M. Linke, T. P. Harty, D. P. L. Aude Craik, D. N. Stacey, A. M. Steaneand, and D. M. Lucas, Hybrid quantum logic and a test of Bells inequality using two different atomic isotopes, Nature (London) **528**, 384 (2015).

[37] D. Hayes, S. M. Clark, S. Debnath, D. Hucul, I. V. Inlek, K. W. Lee, Q. Quraishi, and C. Monroe, Coherent Error Suppression in Multiqubit Entangling Gates, Phys. Rev. Lett. **109**, 020503 (2012).

[38] T. J. Green and M. J. Biercuk, Phase-Modulated Decoupling and Error Suppression in Qubit-Oscillator Systems, Phys. Rev. Lett. **114**, 120502 (2015).

[39] W. Nagourney, J. Sandberg, and H. Dehmelt, Shelved Optical Electron Amplifier: Observation of Quantum Jumps, Phys. Rev. Lett. **56**, 2797 (1986).

[40] P. Neumann, J. Beck, M. Steiner, F. Rempp, H. Fedder, P. R. Hemmer, J. Wrachtrup, and F. Jelezko, Single-shot readout of a single nuclear spin, Science **329**, 542 (2010).

[41] D. Gottesman and I. L. Chuang, Demonstrating the viability of universal quantum computation using teleportation and single-qubit operations, Nature (London) **402**, 390 (1999).

[42] T. P. Harty, D. T. C. Allcock, C. J. Ballance, L. Guidoni, H. A. Janacek, N. M. Linke, D. N. Stacey, and D. M. Lucas, High-Fidelity Preparation, Gates, Memory, and Readout of a Trapped-Ion Quantum Bit, Phys. Rev. Lett. **113**, 220501 (2014).

[43] T. Ruster, C. T. Schmiegelow, H. Kaufmann, C. Warschburger, F. Schmidt-Kaler, and U. G. Poschinger, A long-lived Zeeman trapped-ion qubit, Appl. Phys. B **122**, 254 (2016).

[44] D. J. Larson, J. C. Bergquist, J. J. Bollinger, W. M. Itano, and D. J. Wineland, Sympathetic Cooling of Trapped Ions: A Laser-Cooled Two-Species Nonneutral Ion Plasma, Phys. Rev. Lett. **57**, 70 (1986).

[45] D. P. L. Aude Craik, N. M. Linke, M. A. Sepiol, T. P. Harty, C. J. Ballance, D. N. Stacey, A. M. Steane, D. M. Lucas, and D. T. C. Allcock, High-fidelity spatial and polarization addressing of $^{43}Ca^{+}$ qubits using near-field microwave control, Phys. Rev. A (to be published).